Optimized Signal Processing for High-Resolution FBG Strain Sensing Using a Dual-Comb Interrogator

Optimized Signal Processing for High-resolution FBG Strain Sensing Using a Dual-comb Interrogator

Alejandro Rosado [1,2*], Malhar A. Nagar [3], Minghao Wei [1, 2], Conor McArdle [1], Aleksandra Kaszubowska-Anandarajah [2, 1], Davide Janner [3] and Prince M. Anandarajah [1, 2]

[1] Photonics Systems and Sensing Lab (PSSL), School of Electronic Engineering, Dublin City University, Glasnevin, Dublin 9, Ireland. (*) alejandro.rosado@dcu.ie
[2] CONNECT Research Centre, School of Engineering, Trinity College Dublin, D02 W272, Ireland.
[3] Dipartimento di Scienza Applicata e Tecnologia (DISAT), Politecnico di Torino, Corso Duca degli Abruzzi, 24, 10129, Turin, Italy.

Abstract *A high-resolution sensing system based on a DOFC interrogating a fs-inscribed FBG is presented. Optimized signal processing was employed to obtain sub-με strain resolution (0.32 με) with a dynamic range of 422 με, highlighting the potential for precise and real-time sensing applications.*

Introduction

A fibre Bragg grating (FBG) is a periodic modulation of the refractive index inscribed in the core of an optical fibre, which selectively reflects light at a specific wavelength. They are broadly used as optical sensors in a plethora of applications due to their beneficial properties, such as high sensitivity, compactness and multiplexing capabilities [1]. In particular, femtosecond-laser (fs) written FBGs are attracting increasing research efforts due to their inherent characteristics, such as temperature tolerance and robustness [2,3]. The interrogation/calibration of these sensors typically demands high spectral resolution. However, the use of traditional interrogation approaches for high precision static strain sensing suffers from several limitations [4,5] in terms of resolution, speed or dynamic range, especially pronounced in strain sensors.

Optical frequency combs (OFCs) are made up of an array of equally spaced coherent optical tones in the spectral domain, and are considered as one of the most versatile systems for many diverse applications, including optical interrogation. The broad range of applications across several fields, includes optical telecommunications, atomic clocks, and optical sensing [6]. A commonly used implementation of the OFC for sensing applications is known as the Dual-OFC (DOFC) [7]. This technique exploits the interference of two different OFCs (phase referenced to each other through a common master laser) having two slightly different free spectral ranges (FSRs). When detected, the resulting multi-heterodyne beating produces a down-converted radio frequency (RF) signal, that preserves the optical information of both OFCs in the RF domain. High resolution, precise measurement, real-time acquisition and high dynamic range are some of the attributes associated with this method. Besides, the use of the DOFC significantly simplifies the electronics employed for the detection, eliminating the necessity of moving elements, thereby enhancing stability and integration. Several techniques have been employed for DOFC generation. Among all, gain-switching [12] has become one of the most popular techniques due to its inherent simplicity, its cost-effective implementation with commercially available components, and its potential for integration. This technique relies on a strong modulation of two semiconductor lasers by two RF signals at slightly different frequencies. The combined signal results in a high-quality DOFC, whose performance and mutual coherence can be largely improved by the use of external optical injection [13].

Several approaches for FBG sensing based on DOFCs have been reported, each of them with different advantages and limitations [8,10-11]. Although narrowband FBG interrogation has been successfully demonstrated using DOFCs, extending this approach to broadband FBGs, and more specifically to the fs-written FBGs, may compromise some of the intrinsic benefits associated with this technique, particularly in terms of spectral resolution, which becomes insufficient for the peak tracking of broader spectra.

Here, the implementation of different optimizing algorithms is explored to counteract this effect, enabling accurate FBG shift tracking of broadband FBGs with a comparable precision with their narrowband counterparts. This is accomplished using a DOFC interrogator based on two externally-injected gain-switched lasers (EI-GSL). The results reported in this study successfully demonstrates peak tracking of broadband FBGs through different strategies, all of them capable of following very small strain fluctuations (some less than 0.8 pm) and improving previously reported results [14].

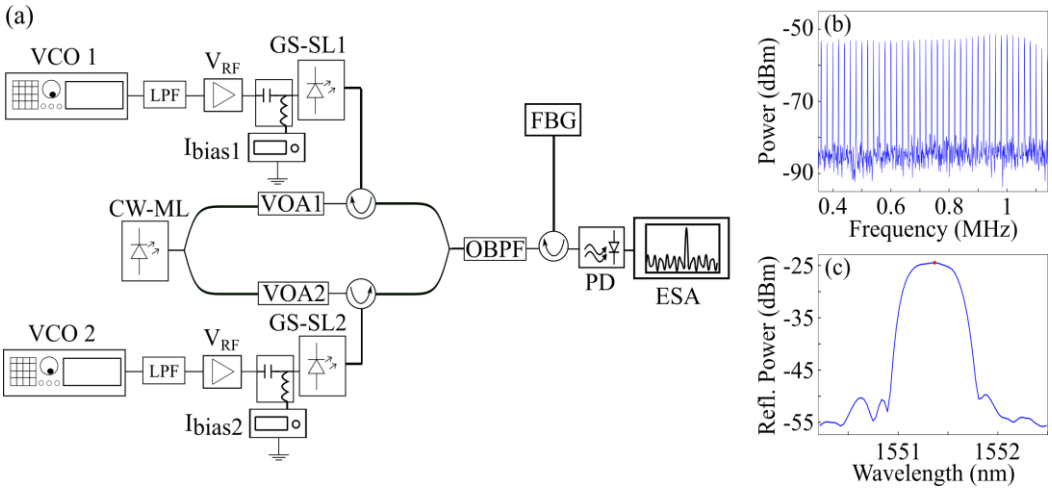

Fig.1a: Experimental setup used for DOFC generation and FBG interrogation. CW-TL: tunable laser in CW operation, VOA: variable optical attenuator, GS-SL: gain-switched slave laser, VCO: voltage-controlled oscillator, OBPF: optical bandpass filter, FBG: fiber Bragg grating, PD: photodetector, ESA: electrical spectrum analyzer; **Fig.1b:** Reference RF comb resulting from the down-conversion of the photodetected optical signal; **Fig.1c:** Reflection spectra of the FBG.

Experimental setup

The DOFC generator consists of two optically injected Fabry-Perot (FP) lasers, gain-switched at the repetition rates of 1 and 0.99998 GHz using sinewaves generated by two synthesizers. The output of the synthesizer is filtered and then amplified to obtain high-power RF signals with high purity. The master laser, a commercial tunable laser with a linewidth of 75 kHz, is optically attenuated prior to its injection into two circulators, to ensure high-quality OFC generation. Then, both OFCs are combined and directed through a band-pass optical filter and the FBG by means of a circulator (for the reflection spectra measurements). The resulting signal from the FBG is photodetected and analysed using an electrical spectrum analyser (ESA). A sample of the down-converted RF comb is provided in Fig.1b. The employed FBG for these experiments has a central wavelength of 1551.38 and a 3-dB bandwidth of 0.5 nm. Its reflected spectrum is depicted in the Fig.1c. One of the terminals of the FBG was mounted over a piezoelectric transducer (PZT) connected to a servo-controller, which induces strain variations in the FBG, ranging from nano to micro strains. The strain induced by the PZT controller was progressively increased by applying controlled displacements in the range of 10 nm to 5 μm, corresponding to strain variations spanning from 33.33 nε to 32.68 με, respectively.

Experimental calibration and discussion

The calibration process was carried out in the following steps: firstly, we measured the RF comb on the ESA without any induced strain, as a reference. After that, we progressively increased the controlled strain in the FBG, whilst measuring the resulting RF comb. The different values of the strain affected the resulting RF comb by changing its shape and central frequency. Once all the measurements were completed, the FBG shift of the reflected RF comb (and therefore of the FBG) is extracted, through the different algorithms and converted into optical frequencies. The conversion between RF and optical frequencies is given by:

$$f_{opt\text{-}FBG} = f_{inj} - \left(\frac{f_R}{f_{off}}\right)(f_{RF\text{-}samp} - f_{RF\text{-}ref}) \qquad (1)$$

where f_{inj} is the frequency of the injected laser (193.177 THz), f_R is the FSR of the 1st OFC (f_R = 1GHz), f_{off} is the FSR difference between two combs, f_{off} = 20 kHz; and $f_{RF\text{-}samp}$ and $f_{RF\text{-}ref}$ the retrieved frequencies of the RF comb for each value of strain, and the reference, correspondingly. Finally, to obtain the Bragg wavelength, $f_{opt\text{-}FBG}$ is converted into wavelength.

The first employed retrieval algorithm was the hyperbolic tangent fitting (HTF). This algorithm fits the amplitude of all the tones of the RF comb to the following equation:

$$f(x) = a + b\tanh(c(x\text{-}d)), \qquad (2)$$

where a denotes the baseline power level, b is the transition amplitude, c the steepness of the transition, and d the central frequency. An example of this method is provided in Fig.2(a), where the induced strain corresponds to 127με. When comparing the RF combs for two cases: unstrained (Fig. 1(b)) and strained FBG (Figs. 2(a) or 2(b)), it can be seen that, when the FBG is strained its reflection profile shifts towards lower frequencies, corresponding to higher wavelengths. The wavelength of the FBG has been retrieved from "d" of Eq. (2) and plotted in Fig. 2(d), for different values of strain. A sensitivity of 1.29 pm/με and an R^2 = 0.98 for applied strain increments of 18.18 με were obtained with this method.

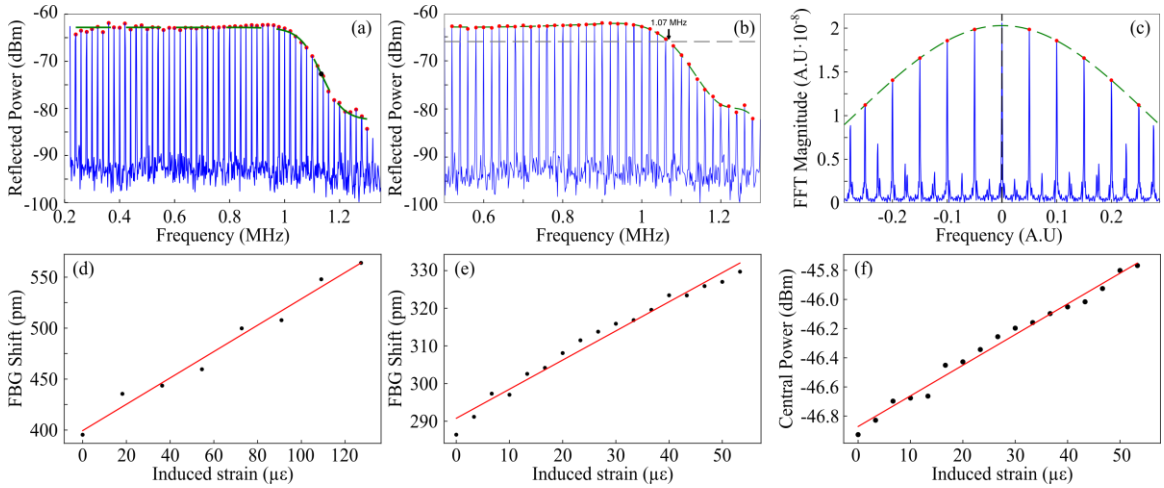

Fig.2: Top: (a) and (b): measured RF comb at different conditions of calibrated strain (blue) and its corresponding fitting according to the chosen algorithm (in red); (c) FFT of the RF comb (in blue) and its corresponding fitting to a gaussian line shape. Bottom: corresponding calibration plot of each retrieval algorithm.

The second algorithm to retrieve the central frequency of the RF comb is the spline fitting (SF) with constant power monitoring. Here, the amplitudes of the RF comb lines were fitted using a univariate spline fitting function expressed as:

$$s(f) = \sum_{i=0}^{N} c_i \cdot B_i(f), \qquad (3)$$

where $B_i(f)$ is the basis of the spline functions, and c_i is the coefficient determined through the fitting process. To monitor the position of the FBG under varying strain conditions, we employed as a reference the frequency coordinates corresponding to the intersection points between the fitted splines and a fixed threshold set at -66 dBm, a value empirically optimized to enhance linearity while preserving a high signal-to-noise ratio. An example of this fitting, for a 52 με applied to the FBG, is provided in Fig. 2(b). The results of the strain calibration using this algorithm are presented in Fig. 2(e). The obtained linear slope of Fig. 2(e) corresponds to a sensitivity of 0.77 pm/με and a R^2 = 0.98 for applied strain increments of 3.3 με.

The last used method for frequency retrieval uses the fast Fourier transform (FFT) of the resulting RF comb. This method reveals a power distribution that can be approximated to a Gaussian profile and whose maximum amplitude depends exclusively on the applied strain (Fig. 2(c)). The evolution of the Gaussian amplitude, when the calibrated strain is changed, is shown in Fig. 2(f). The obtained linear slope of Fig. 2(c) corresponds to a sensitivity of 0.0210 dBm/με with a R^2 = 0.99 for applied strain increments of 3.3 με.

Finally, we benchmarked strain measurements using a state-of-the-art commercial interrogator (with 1000 averaged traces, a data processing rate of 2.5Hz and an integration time of 3s). To ascertain the quality of each algorithm, we have determined the minimum attainable resolution (R), defined as the ratio of the standard deviation of the linear fitting of each algorithm and its retrieved slope, an estimation of the minimum measurable strain with each method. A summary of the main parameters of each algorithm in comparison with those results obtained with the commercial interrogator are shown in Table 1. The results show that different methods deliver different benefits/performance. E.g., HTF can be used for higher strain regimes (≥ 3 με) because it reliably captures the steep transitions in the reflection spectrum. SF on the other hand, is particularly effective at low strains (≤ 3 με) due to its noise-smoothing properties and precise threshold detection. Similarly, FFT-based Gaussian fitting efficiently isolates the main spectral component from the PSD data, supporting accurate tracking of minute frequency shifts.

Tab. 1: Summary of the obtained relevant parameters of each retrieval algorithm.

Method	σ_c	S	R (με)
M1: HTF	8.19 pm	1.29 pm/με	6.34
M2: SF	0.32 pm	0.77 pm/με	0.42
M3: FFT	0.02 dB	0.07 dB/με	0.32
Commercial	0.56 pm	1.18 pm/με	0.48

Conclusions

Here, we show the first comprehensive demonstration of DOFC-FBG interrogation techniques applied to standard fs-written gratings for high-resolution FBG strain sensing. By optimizing signal processing techniques, sensitivities around 1 pm/με with a higher degree of linearity (R^2 > 0.98) were achieved, surpassing the performance of a commercial interrogator for static strain sensing, and obtaining lower minimum attainable resolutions (0.32 με, corresponding to strain fluctuations of 0.8 pm), paving the way for its use in advance sensing applications that requires ultra-fine strain measurements.

Acknowledgements

This research work was supported in part by the Research Ireland/European Regional Development Fund (13/RC/2077/P2) and NATO SPS.MYP.G6056 projects.

References

[1] 'Polymer-Based Optical Guided-Wave Biomedical Sensing: From Principles to Applications'. Accessed: Dec. 17, 2024. [Online]. Available: https://www.mdpi.com/2304-6732/11/10/972

[2] B. Xu et al., 'Femtosecond laser point-by-point inscription of an ultra-weak fiber Bragg grating array for distributed high-temperature sensing', Opt. Express, OE, vol. 29, no. 20, pp. 32615–32626, Sep. 2021, https://doi.org/10.1364/OE.437479

[3] J. He, B. Xu, X. Xu, C. Liao, and Y. Wang, 'Review of Femtosecond-Laser-Inscribed Fiber Bragg Gratings: Fabrication Technologies and Sensing Applications', *Photonic Sens*, vol. 11, no. 2, pp. 203–226, Jun. 2021, https://doi.org/10.1007/s13320-021-0629-2

[4] M. M. M. Werneck, R. C. S. B. Allil, and F. V. B. de Nazaré, 'Interrogation Techniques of Fiber Bragg Gratings', in Fiber Bragg Gratings: Theory, Fabrication, and Applications, vol. TT114, SPIE, 2017, pp. 65–77. https://doi.org/10.1117/3.2286558.ch6

[5] Q. Liu, T. Tokunaga, and Z. He, 'Realization of nano static strain sensing with fiber Bragg gratings interrogated by narrow linewidth tunable lasers', *Opt. Express, OE*, vol. 19, no. 21, pp. 20214–20223, Oct. 2011, https://doi.org/10.1364/OE.19.020214

[6] N. R. Newbury, 'Searching for applications with a fine-tooth comb', Nature Photon, vol. 5, no. 4, pp. 186–188, Apr. 2011, https://doi.org/10.1038/nphoton.2011.38

[7] Ian Coddington, Nathan Newbury, and William Swann, "Dual-comb spectroscopy," Optica 3, 414-426 (2016), https://doi.org/10.1364/OPTICA.3.000414

[8] Naoya Kuse, Akira Ozawa, and Yohei Kobayashi, "Static FBG strain sensor with high resolution and large dynamic range by dual-comb spectroscopy," Opt. Express 21, 11141-11149 (2013) https://doi.org/10.1364/OE.21.011141

[9] R. Zhang, Z. Zhu, and G. Wu, 'Static pure strain sensing using dual–comb spectroscopy with FBG sensors', Opt. Express, OE, vol. 27, no. 23, pp. 34269–34283, Nov. 2019, https://doi.org/10.1364/OE.27.034269

[10] J. Guo, Y. Ding, X. Xiao, L. Kong, and C. Yang, 'Multiplexed static FBG strain sensors by dual-comb spectroscopy with a free running fiber laser', Opt. Express, OE, vol. 26, no. 13, pp. 16147–16154, Jun. 2018, https://doi.org/10.1364/OE.26.016147

[11] J. E. Posada-Roman, J. A. Garcia-Souto, D. A. Poiana, and P. Acedo, 'Fast Interrogation of Fiber Bragg Gratings with Electro-Optical Dual Optical Frequency Combs', Sensors, vol. 16, no. 12, Art. no. 12, Dec. 2016, https://doi.org/10.3390/s16122007

[12] P. M. Anandarajah *et al.*, 'Generation of Coherent Multicarrier Signals by Gain Switching of Discrete Mode Lasers', *IEEE Photonics Journal*, vol. 3, no. 1, pp. 112–122, Feb. 2011, https://doi.org/10.1109/JPHOT.2011.2105861

[13] Eamonn P. Martin *et al.*, "Stability Characterisation and Application of Mutually Injection Locked Gain Switched Optical Frequency Combs for Dual Comb Spectroscopy", IEEE/OSA Journal of Lightwave Technology, vol. 41, no. 13, pp. 4516-4521, July 2023. https://doi.org/10.1109/JLT.2023.3255550

[14] X. Zhao, Q. Li, S. Yin, J. Chen, and Z. Zheng, 'Dual-Comb Dynamic Interrogation of Fiber Bragg Grating With One Mode-Locked Fiber Laser', IEEE Sensors Journal, vol. 18, no. 16, pp. 6621–6626, Aug. 2018, https://doi.org/10.1109/JSEN.2018.2852846